DRUG DEVELOPMENT AND INDUSTRIAL PHARMACY, 21(2), 199-214 (1995)

LACTOSE TEXTURE MONITORING DURING COMPACTING

I. MECHANICAL PROPERTIES AND TEXTURE PARAMETERS

Colette Mbali-Pemba, Dominique Chulia
Laboratoire de Pharmacie galénique, Faculté de Pharmacie,
2, rue Docteur Marcland - 87025 Limoges, France

SUMMARY

Mercury porosimetry has been found to be an effective method of studying the porous texture of compacts (1). The authors used this method to differentiate between materials on the basis of interparticular pore volume and pore surface area. The cohesive properties of eight lactoses were studied from their resistance to simple compaction and discussed with regard to the change in their texture as a function of pressure. A technological classification is proposed.

INTRODUCTION

Lactose is an excipient which is commonly used in pharmaceutical formulations, notably in tablets, where it is used as a diluent or binder, depending on its rheological and mechanical properties and the conditions under which it is used. The modes of densification and cohesion acquisition of eight lactoses - with differing technological properties - have been compared and the texture of the compacts obtained under various confinement pressures has been investigated in order to determine the physical parameters required for high quality results.

MATERIALS AND METHODS

Eight lactoses were studied, and their physicochemical, rheological and mechanical characteristics had been investigated in a previous study (2).

- lactose Fast Flo	FF
- lactose DCL 11	DCL 11
- lactose DCL 21	DCL 21

- tablettose	Tab
- lactose Extra Fin Cristaux	EFC
- lactose Merck	M
- lactose Poudre Fine	PF
- lactose Impalpable	Pl

The FF, DCL 11, Tab, M, EFC, PF and Pl lactoses are α monohydrates and an amorphous phase was detected in FF and DCL 11. DCL 21 was the only β anhydrous lactose.

1-1. Scanning Electron Microscopy

The lactoses were scanned under an EMS electron microscope (Hitachi S-2500) in order to assess the state of the surface and form of their particles.

1-2. Compaction

Each lactose was subjected to single axis compaction in a cylindrical cell with a diameter of 2 cm and a height of 6 cm, using a Seditech press (at a compaction rate of 1.14 mm/min).

Six compaction pressures, P_C, were selected ranging from 100 to 600 bars (1 bar = 0,1 MPa). The resistance to simple compaction, R, was determined in order to evaluate the cohesion of the materials; to do this, the compacts were unmoulded and broken up by applying a vertical force, i.e. along the same axis as the compaction force had been applied (at a rate of 0.38 mm/min).

We adopted Gonthier's model (3), equation 1, which is similar to the first order model proposed by Ryshkewitch (4):

$$R = R_\infty (1-n)^\gamma \qquad \text{(Eq1)}$$

where:

n = porosity calculated after eliminating the stress

R = resistance of the compact (bar)

R_∞ = resistance towards which R tends when n tends towards 0 (bar)

The constant, γ, is used to assess the difficulty experienced by the substance in acquiring cohesion. The higher γ, the more the porosity impedes the capacity of R to reach R_∞.

1-3. Mercury Intrusion Porosimetry

The compacts produced under 100, 300 and 600 bar were subjected to a study of texture. The porosity was determined using a 9300 Micromeretics mercury porosimeter, operating in a pressure range of between 10 mbar and 2070 bar.

Two measurement stations were used to cover this range:

- a low pressure system: operating between 10 mbar and 2 bar. The increments in pressure and equilibrium time were checked manually by the operator;

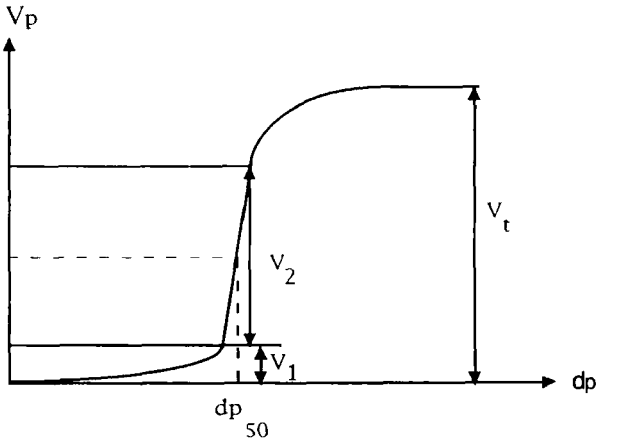

FIGURE 1
Diagram of a Porogram

- high pressure system: operating between 2 bar and 400 bar as no significant change was detected above this. In this case, the increments in pressure and time were checked automatically.

The volume of the penetrometer (measurement cell) in which the upper third of the compact was placed, was equal to 15 cm^3. The cell and its contents were placed in the low pressure system and the gas eliminated from the sample at ambient temperature under a residual pressure of a few pascal. A check was carried out to make sure that the elimination of water had not affected the shape or size of the particles. The penetrometer was then brought into contact with the mercury in the high pressure system.

Mercury, a liquid metal, with a high surface tension (ω), does not wet solid surfaces. To force mercury into the pores of the solid, a pressure (P_{Hg}) has to be applied which is greater the smaller the pores.

This pressure is increased by successive steps, and the volume of mercury which has entered the sample after each increase is measured. It is therefore presumed that all the pores communicate with one another.

The experimental data are the volume of mercury which as penetrated (V) as a function of the pressure applied (P_{Hg}): $V = f(P_{Hg})$.

These data are usually given in the form of a porogram, the volume of mercury as a function of the diameter of the pores: $V = f(d_p)$. The mercury yields only the diameter of the entrance of the pore, but a model is assumed of cylindrical pores forming a perfect network in which the mercury is forced to go through a large pore in order to reach a smaller one.

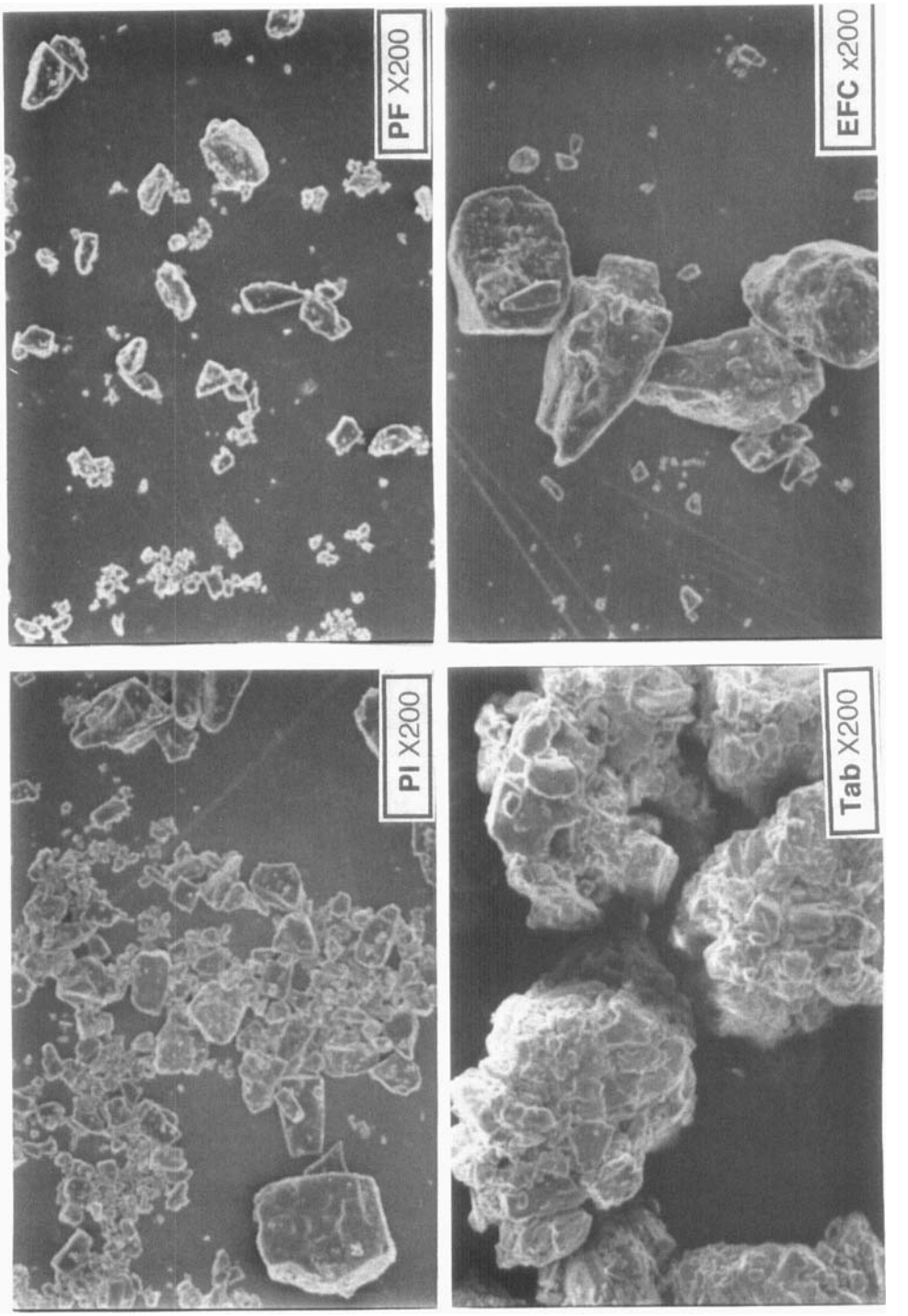

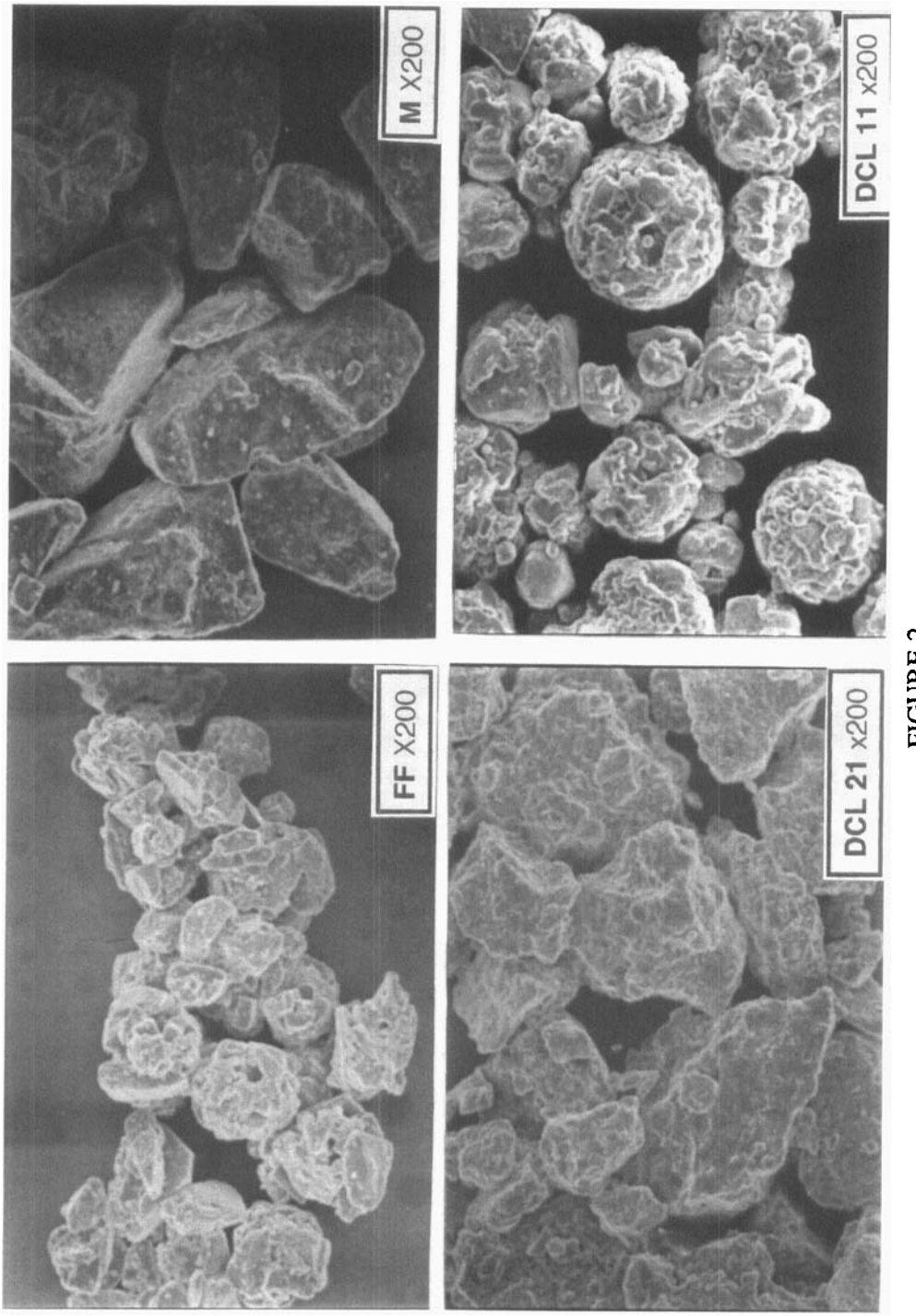

FIGURE 2
Morphology of the Lactoses tested

The diameter is calculated from the mercury penetration pressure, using Washburn's equation (5, 6, 7):

$$dp = -\frac{4\omega\cos\theta}{P} \qquad \text{(Eq2)}$$

where
d_p : diameter of the pores
P : pressure required for the mercury to penetrate into the pores
ω : surface tension of the mercury (484 dynes/cm)
θ: mercury/solid contact angle (130°)

From the porogram (Figure 1) the following can be read off:
- the interparticular pore volume in the confined state, V_2 (cm^3/g) = V_t-V_1, where V_1 corresponds to the confinement and particular rearrangements;
- the median diameter, d_{p50} in µm, the distribution in volume of the interparticular pores.

Taking for $\overline{P_i}$ the mean pressure of mercury between two consecutive and close experimental points:

$$\overline{P_i} = \frac{(P_i + P_{i+1})}{2} \qquad \text{(Eq3)}$$

ΔV_i is the change in volume during this increase in pressure.
Using a model of cylindrical pores, and assuming that the entire pore volume is distributed in a single long pore, its length, L, is calculated.

$$L = \frac{4V}{\pi D^2} \qquad \text{(Eq4)}$$

RESULTS

2-1. SEM Scans

The various scans (Figure 2) confirm that the lactoses tested take the following form:

FF and DCL 11 are atomised substances which take the form of open and spherical agglomerates.
DCL 21 consists of large particles constituted of more angular agglomerates.
Tab consists of small, very fragile crystals which are organised to form very large agglomerates.

EFC consists of clumped large crystals plus a few fine ones.
M consists of angular clumps of large crystals.
PF takes the form of fine crushed particles.
Pl takes the form of particles consisting of platelets of varying size.

2-2. Resistance of the Compacts

Figure 3 shows the change in resistance, R, of the compact of each lactose with pressure and Table 1 indicates the values of the parameters, R_{600}, the resistance of the compacts compacted at 600 bar, R_∞ and γ of the porosity/resistance model.

2-3. Porosity

The increase in the compacting pressure (P_c) leads to a reduction in the porosity of the compacts, which was clearly different in the various lactoses (Figure 4).

Figure 5 shows the derivated curves obtained for all eight lactoses compacted at 600 bar.

This yields a pairwise classification in terms of size and volume of the main pores:

FF and DCL 11; M and EFC; Tab and DCL 21; PF and Pl

INTERPRETATION

Figures 6 and 7 show the change in resistance, R, with the total length, L, of the theoretical pores and with the total pore volume.

From Figures 3, 6 and 7, the following groups can be identified:

- FF and DCL 11 rapidly acquire cohesion: dR/dP is high, dR/dV is high, but the length of the pores does not show any significant change;
- PF and Pl acquire cohesion slowly: dR/dP low, dR/dV low, L increases sharply;
- DCL 21, Tab, EFC and M are intermediate between the two previous groups, but there are differences: the cohesion of DCL 21 makes it behave in a similar fashion to FF-DCL 11 as the pressure tends towards 600 bar. However, cohesion is acquired earlier by DCL 21 (the value of R_{100} is higher). Tab, EFC and M resemble PF and Pl by the limited acquisition of resistance.

Differences in mechanisms can be seen from the differences in Figure 6, which clearly reveal the subgroups DCL 21-Tab and EFC-M

Figure 8 shows that there is a relationship between γ and R_{600}.

FF and DCL 11 have a low value of and within the range of pressure explored, densification is achieved which gives a high value for R_{600}.

DCL 21 and M have a low γ, but DCL 21 gains more cohesion than M.

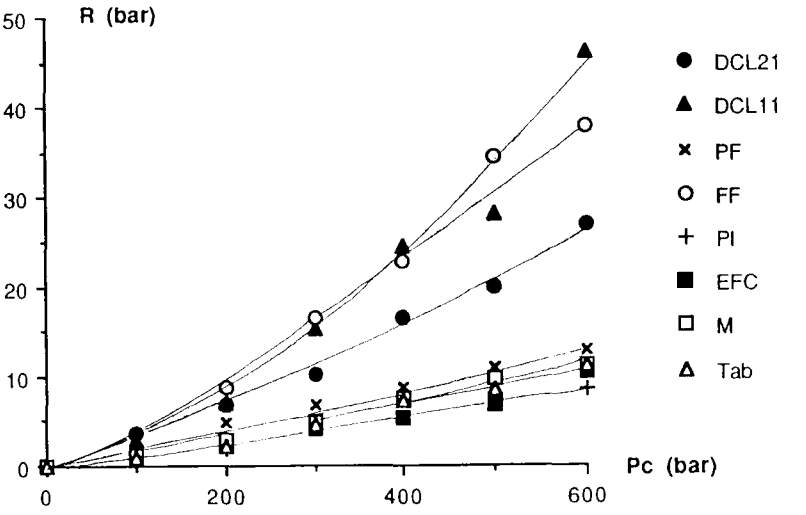

FIGURE 3
Change in the Cohesion of the Compacts

TABLE 1

Rupture parameters

Materials	R600 (bar)	R∞ (bar)	γ
DCL 11	46	718	10
FF	38	1281	11
DCL21	27	210	9,4
PF	13	311	140
M	11	140	12
Tab	11	571	15
EFC	10,5	218	16
PI	8,5	600	18

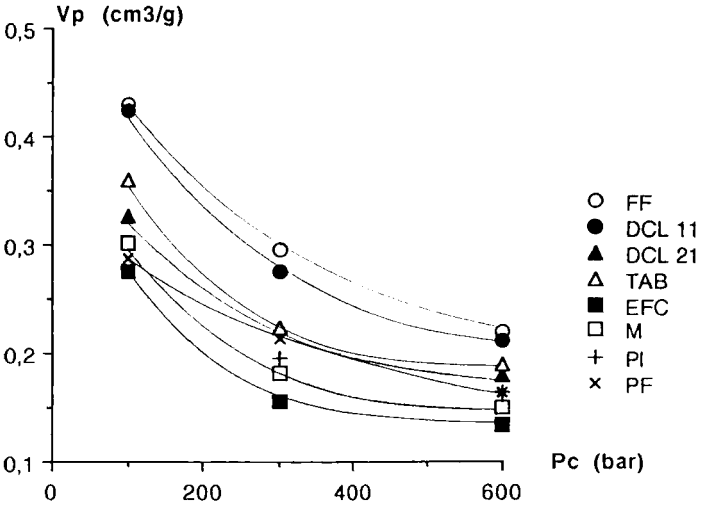

FIGURE 4
Change in Pore Volume with Compacting Pressure

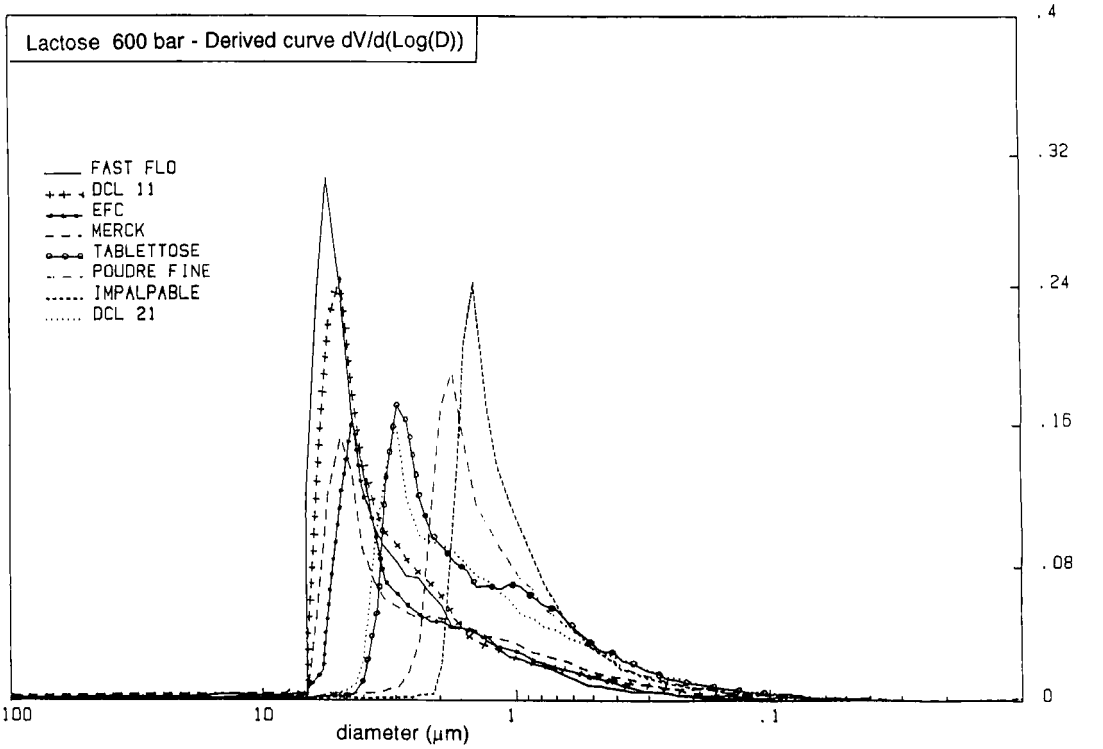

FIGURE 5
Porogram of the Compacts of Lactoses at 600 bar

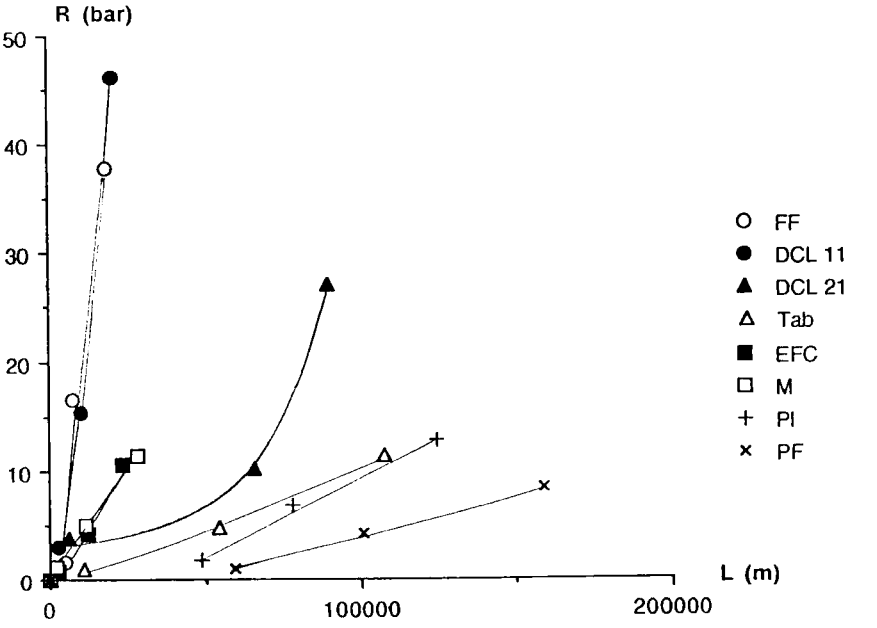

FIGURE 6
Change in resistance with the pore length

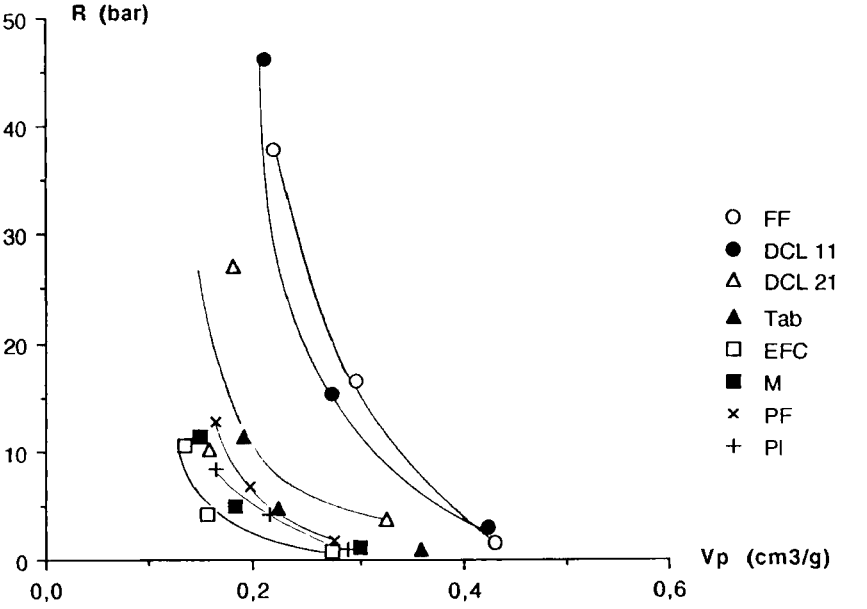

FIGURE 7
Change in resistance with the pore volume

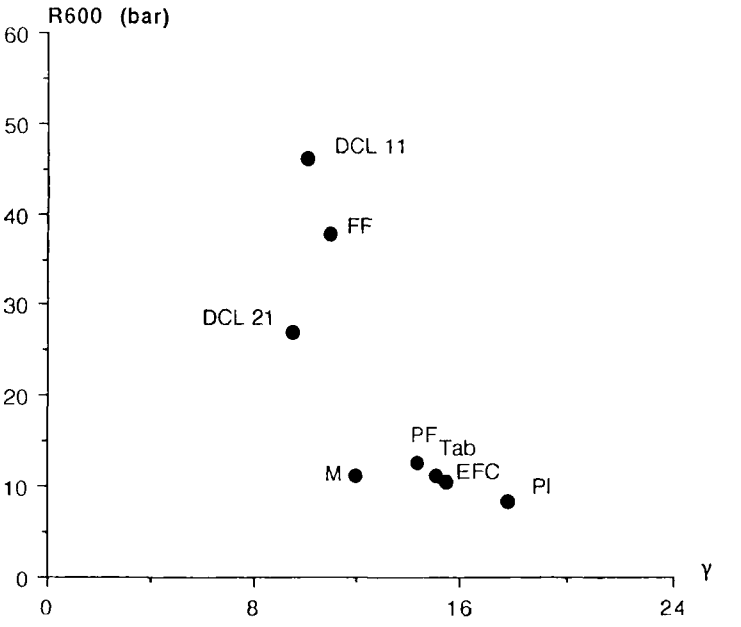

FIGURE 8
Change in the resistance R_{600} with γ

In the case of Tab, EFC, PF and Pl, which have a high value of γ, the densification at 600 bar made it impossible for the resistance to rise above 13 bar.

The lower γ, the sooner resistance develops, because less pore-filling is required to achieve cohesion.

An increase in γ initially results in a closing of the pores followed by the acquisition of resistance.

Figures 9 and 10 show the change in the values of L_{600} and V_{600} with γ.

It is of interest to investigate the relationship between L and γ, knowing that any reduction in V_p is indicative of a rearrangement of the particles and only an increase in L reflects their fragmentation. Pl can be crushed and rearranges itself in response to stress, the length L_{600} is high, indicating numerous fine particles and γ is also a maximum for this product. DCL 11 is resistant to fragmentation (L increases little), it is porous (V_p is high) and it is hard (R is high and γ low). FF and M resist pressure, unlike Tab and PF (L_{600} high). FF maintains porosity which is clearly higher than that of M. Lactose EFC undergoes considerable rearrangement, but without being crushed. DCL 21 is crushable but undergoes little rearrangement as it is resistant to rupture.

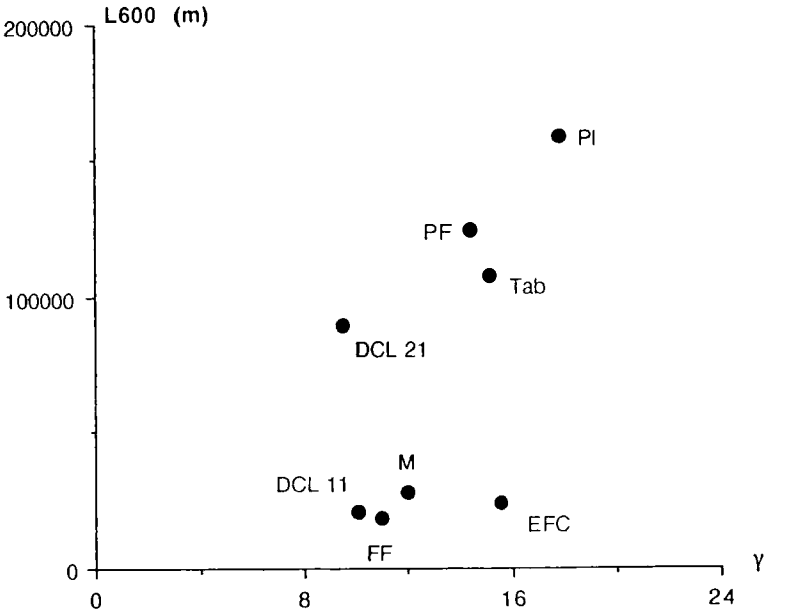

FIGURE 9
Pore length, L_{600}, as a function of γ

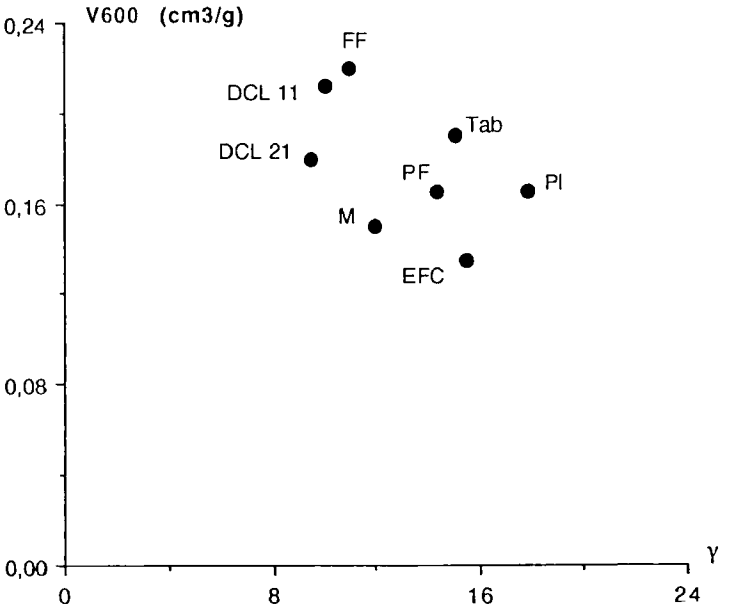

FIGURE 10
Pore volume, V_{600} in function of γ

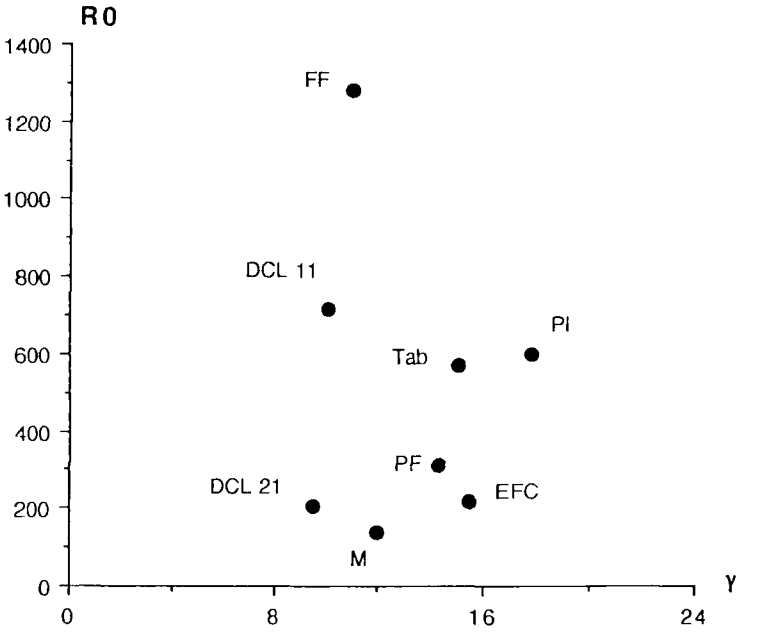

FIGURE 11
R as a function of γ

As we saw in paragraph 1-2, R_∞ is the highest resistance which the material would reach as the porosity tends towards zero. Its change with γ expresses the potentialities of the material (Figure 11), but the actual behaviour during compaction is more closely related to R_{600} and weighted by V_{600}: the substance must acquire cohesion for technological reasons, but it must also maintain porosity for lyoavailability reasons (Figures 12 and 13).

Two substances stand out from the others: FF and DCL 11 as they are hard and readily acquire cohesion (high value of R_{600}). FF would be preferable if the tendency towards cohesion were the sole criterion for choice, as it has a higher R_∞. DCL 21 has a remarkably low γ but a mediocre value of R_∞. However, despite this low value of R_∞, at 600 bar, DCL 21 develops remarkable cohesion compared to the Tab, EFC, M, PF and Pl group of substances, which are less interesting during compaction for a variety of reasons:

- for the four substances Tab, EFC, PF and Pl, γ is high but R_∞ is good for Tab and Pl, acceptable for PF and poor for EFC,
- EFC, as well as having a poor aptitude for cohesion, is distinguished following densification by having the lowest porosity (Figure 13),
- M, due to its low R_∞ and a high degree of rearrangement (Figures 13 and 7).

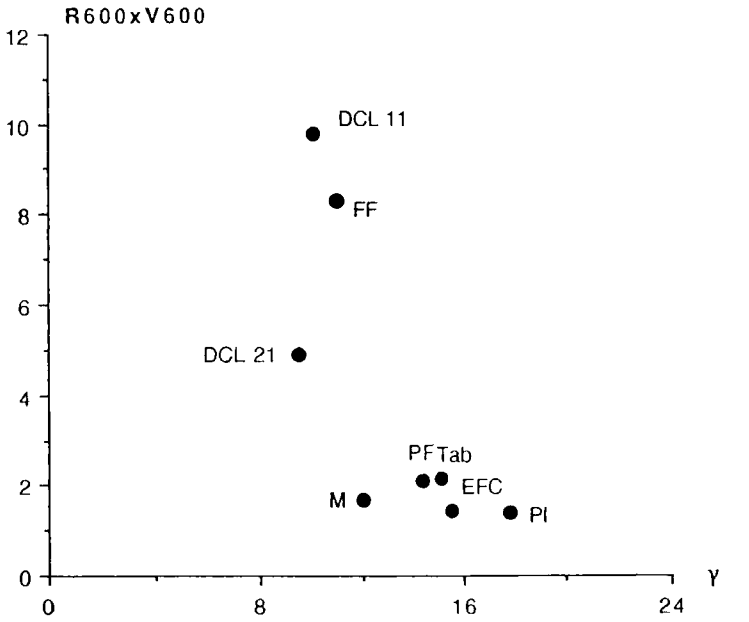

FIGURE 12
R_{600} x V_{600} as a function of γ

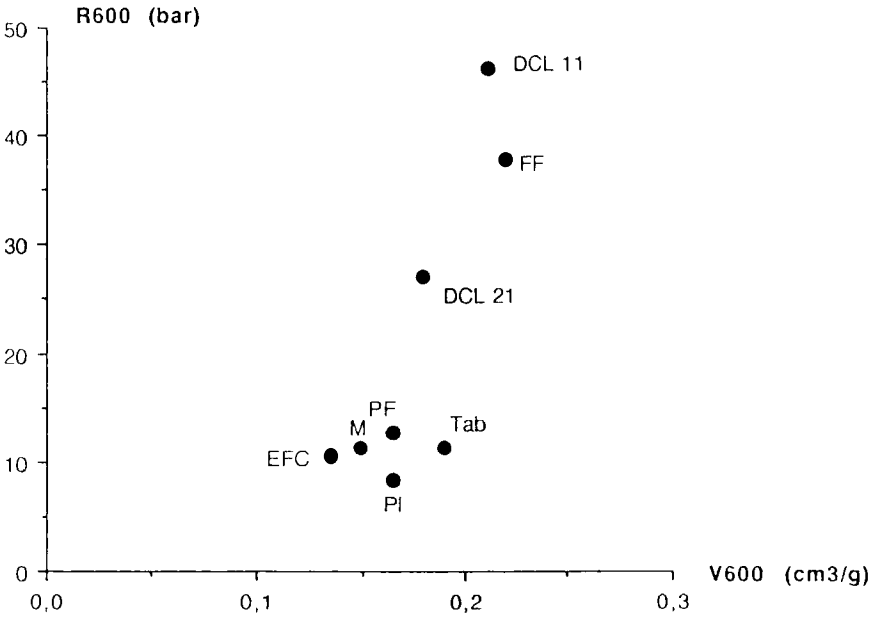

FIGURE 13
Change in R_{600} as a function of V_{600}

A previous study has shown that FF, DCL 11, DCL 21, M and Tab easily flow. EFC has borderline flow properties and the flowability of PF and Pl is poor (2).

Overall consideration of the flowability, cohesion and change in porous texture with pressure confirms the technological superiority of FF, DCL 11 and DCL 21.

CONCLUSION

This study has characterised the behaviour of eight grades of the test substance, lactose, in response to pressure. The capacity of developing cohesion as pressure increases can be expressed by the parameter γ, whereas the maximum potential cohesion is contained in R_∞.

Texture analysis of the compacts by mercury porosimetry has also demonstrated the role of crystallographic and textural parameters on compressibility. Substances which the manufacturing process has textured in the form of spherical agglomerates are the most effective: these are Fast Flo lactose and DCL 11 lactose. The change in the porosity of the compacts and the quality of the particle bonds contained in γ can then be used to distinguish lactose DCL 21. In this case, the performance during compaction is due more to the structure effect - DCL 21 is a β anhydrous lactose - than to the texture effect.

The study of the texture of compacts can also be used to provide selection criteria with regard to the residual porosity following compaction and the lyoavailability.

The porous characteristics of the compacts at 600 bars (total volume, surface area, length) and their change from the porosity at 200 bars, shed further light on an understanding of the mechanisms involved. In order to elucidate the above interpretations, which are based on global values of porosity, an analysis by group of pores will be described in a subsequent study.

ACKNOWLEDGEMENTS

The authors would like to thank D. Tanguy (Rhône-Poulenc Industrialisation, Décines, France) for having provided them in using the mercury porosimeter and M. Deleuil (Rhône-Poulenc Rorer Santé, Antony, France) for the discussion of the results.

REFERENCES

1. H. Vromans, G.K. Bolhuis, C.F. Lerk ,K.D. Kussendrager and H. Bosch , Studies on tableting properties of lactose - VI. Consolidation and compaction of spray-dried amorphous lactose, Acta Pharm. Suec., **23**, 231 (1986).

2. C. Mbali-Pemba, D. Chulia and M. Deleuil , Analysis of the compressibility of particulate materials, physical and mechanical characterization of different grades of lactose., 6° Cong. Int. Technol. Pharm., **1**, 410 (1992).

3. Y. Gonthier, Contribution à l'étude du comportement mécanique des poudres pharmaceutiques sous pression, Thèse de Doctorat, Grenoble, n°7, 1984.

4. E.Ryshkewitch, Compression strength of porous sintered aluminia and zirconia, J. Am. Ceram. Soc., **36**, 65 (1953).

5. M. Riippi, J. Yliruusi, J. Kiesvaara and T. Niskanen, The use of high pressure mercury porosimetry in determination of the porosity of Erythromycin acistrate tablets compressed with different compression forces, 10th Pharm. Techn. Conference, Bologne (1991).

6. E.J. Garboczi, Mercury porosity and effective networks for permeability calculations in porous materials, Powder technol., **67**, 121 (1991).

7. D. Chulia, M. Deleuil, M. Sautel and C. Mbali-Pemba, Modelisation of powders behaviour under pressure: characterization of DC grade active principles, 6° Cong. Int. Technol. Pharm., **4**, 140 (1992).